

Newtonian Analysis of Gravitational Waves from Naked Singularity

Ken-ichi Nakao¹, Hideo Iguchi² and Tomohiro Harada³

¹*Department of Physics, Osaka City University*

Osaka 558-8585, Japan

²*Department of Earth and Space Science, Graduate School of Science, Osaka University*

Toyonaka, Osaka 560-0043, Japan

³*Department of Physics, Waseda University*

Oh-kubo, Shinjuku-ku, Tokyo 169-8555, Japan

Spherical dust collapse generally forms a shell focusing naked singularity at the symmetric center. This naked singularity is massless. Further the Newtonian gravitational potential and speed of the dust fluid elements are everywhere much smaller than unity until the central shell focusing naked singularity formation if an appropriate initial condition is set up. Although such a situation is highly relativistic, the analysis by the Newtonian approximation scheme is available even in the vicinity of the space-time singularity. This remarkable feature makes the analysis of such singularity formation very easy. We investigate non-spherical even-parity matter perturbations in this scheme by complementary using numerical and semi-analytical approaches, and estimate linear gravitational waves generated in the neighborhood of the naked singularity by the quadrupole formula. The result shows good agreement with the relativistic perturbation analysis recently performed by Iguchi et al. The energy flux of the gravitational waves is finite but the space-time curvature carried by them diverges.

PACS number(s): 04.25.Nx, 04.30.Db, 04.20.Dw

I. INTRODUCTION

General relativity predicts that gravitational collapse of massive objects leads to space-time singularities in rather general circumstances in our universe [1–3] and such singularities might be accompanied with the blow up of physical quantities (energy density, pressure and curvature of space-time, etc). The known physical laws including general relativity itself will break down in the neighborhood of the space-time singularity and hence the quantum theory of gravity is believed to be necessary to describe the physical phenomena in such a region.

One of the important issues is whether the space-time singularities formed in our universe are visible or not for the observer (us) far from the region where the gravitational collapse occurs. The cosmic censorship conjecture proposed by Penrose gave a strong motivation to investigate this problem [4]. Roughly speaking, this conjecture states that the singularity is not visible for any observer if it is resulted from physically reasonable initial conditions. However, this conjecture has not yet been proven. Rather candidates of the counterexample of this conjecture have been found.

The simplest example is the gravitational collapse of spherically symmetric dust fluid. There is an exact solution of Einstein equations for this case; the so-called Lemaître-Tolman-Bondi (LTB) solution. After Eardley and Smarr have pointed out the occurrence of a central shell focusing naked singularity of marginally bound dust collapse [5], several theoretical efforts revealed the genericity of the shell focusing naked singularity formation in the LTB solution [6–10]. There are several researches for more general spherically symmetric system and those revealed that non-vanishing pressure does not necessarily prevent the formation of the central shell focusing naked singularity [11–14].

On the other hand, there are not so much researches for non-spherical systems as the spherically symmetric cases since general analytic approach is impossible. Nakamura et al. and Nakamura and Sato performed numerical simulations for axisymmetric perfect fluid system [15,16]. Their results suggest that naked singularities might be formed

if the initial internal energy of the fluid elements is very small and initial configuration is sufficiently elongated. This result is consistent with the hoop conjecture proposed by Thorne, which states that black holes with horizons form when and only when a mass M gets compacted into a region whose circumference in every direction is $C \gtrsim 4\pi M$ [17]. Shapiro and Teukolsky also performed numerical simulations for the axisymmetric collision-less-particle system and showed a possibility of naked singularity formation which is also consistent with the hoop conjecture [18]. The critical behavior of the axisymmetric gravitational waves is also a candidate of the naked singularity formation [19]. An example which can be investigated analytically is the shell focusing naked singularity formation in the Szekeres solution [20]. Anyway, even in the non-spherical cases, there are several examples of naked singularity formation.

There might be readers who state that numerical examples can not be regarded as candidates of naked singularity formation since the numerical simulation can not reveal the global structure of the space-time and further can not deal with infinite quantities (the numerical technique recently proposed by Hübner might be able to avoid this difficulty [21]). However, the present authors would like to stress that if the region of sufficiently high energy, large pressure and large space-time curvature is visible from an observer far from the region, it should be regarded as a naked singularity. The region with extremely large physical quantities will be described by the quantum theory of gravity which is little known and hence such region is equivalent to a space-time singularity in practical sense.

An important point of view for the naked singularity formation process has been proposed by Nakamura et al. [22]. They pointed out that the visible strong curvature region may be a candidate of strong gravitational wave sources. Gravitational waves generated in such a region will propagate out from there since there is no event horizon. From this point of view, Chiba investigated cylindrical gravitational collapse but his result is not consistent to the Nakamura et al's conjecture [23]. The numerical simulations by Shapiro and Teukolsky essentially agrees with Chiba's result with respect to the gravitational radiation. However, we should be concerned about the numerically covered domain since the gravitational waves might be emitted from just the neighborhood of the naked singularity. Recently, present authors investigated the behavior of aspherical perturbations in the LTB space-time and showed that the Weyl curvature of even mode perturbations corresponding to outgoing gravitational waves diverges [24]. Although this result was obtained by numerical integration of linearized Einstein equations, the numerical stability is guaranteed much better than that of the numerical simulation of full Einstein equations. Further, linearized Einstein equations were solved as the characteristic initial value problem and hence the numerically covered domain of the space-time by this analysis is much wider than the previous two numerical simulations. The results of the linear perturbation analysis of the LTB space-time suggest that gravitational waves will be emitted in the formation process of naked singularities.

The purpose of the present paper is to re-analyze the dynamics of perturbations of the LTB space-time in the framework of the Newtonian approximation. In order that the singularity of the spherically symmetric space-time is naked, "the gravitational potential" $2M/R$ is smaller than unity in the neighborhood of the singularity, where M is the Misner-Sharp mass function and R is the areal radius. The central shell focusing naked singularity of the LTB space-time satisfies this condition and further the gravitational potential vanishes even at this singularity. The speed of the dust fluid is also much smaller than the speed of light before and at the central shell focusing naked singularity formation. Therefore the Newtonian approximation seems to be available, even though the space-time curvature is infinite at the singularity. The advantage of the Newtonian approximation scheme is that the dynamics of perturbations of the dust fluid and gravitational waves generated by the motion of the dust fluid are separately estimated; the evolution of the perturbations of the dust fluid are obtained by the Newtonian dynamics and the gravitational radiation is obtained by the quadrupole formula. Hence the semi-analytic estimate of the gravitational radiation due to the matter perturbation of the LTB space-time is possible if we adopt the Newtonian approximation. The results of the Newtonian perturbation analysis well agrees with the relativistic perturbation analysis by the present authors. This suggests that the Newtonian analysis will be a powerful tool in the analysis of some category of naked singularity. However, we should stress that the neighborhood of the naked singularity is not Newtonian in ordinary sense, because there is indefinitely strong tidal force. Further, studies of quantum effects have revealed that the violent quantum particle creation occurs in this space-time [25–29]. The particle creation is just a highly relativistic phenomenon. The Newtonian approximation scheme is available to describe the dynamics of the neighborhood of the naked singularity but the situation is not Newtonian.

This paper is organized as follows. In Sec.2, we briefly review the LTB solution. In Sec.3, we consider the Newtonian approximation of a spherically symmetric dust collapse and show the relation between the Eulerian, Lagrangian and synchronous-comoving (SC) coordinate systems in this approximation scheme. Further in this section, we show the validity of the Newtonian approximation scheme even in the neighborhood of the central shell focusing naked singularity as long as we adopt the Eulerian coordinate system. The basic equations for the even mode of perturbations are presented in Sec.4. In order to estimate the gravitational radiation generated by aspherical perturbations of dust fluid, we need the knowledge about mass-quadrupole moment. We show an explicit expression of the quadrupole moment in Sec.5. Then we show the numerical calculation in Sec.6 and the asymptotic behavior of the mass-quadrupole moment is presented in Sec.7. Finally, Sec.8 is devoted for summary and discussion.

In this article, we adopt $G = c = 1$ unit and basically follow the convention and notation in Ref. [30]. The Greek indices mean components of tensors, while the Latin indices except for ℓ and m represent a type of a tensor. We use the sub- or super-scripts ℓ and m to denote spatial components of tensors.

II. THE SPHERICALLY SYMMETRIC DUST COLLAPSE

In general, the gravitational collapse of a spherical dust ball produces a shell focusing naked singularity at the symmetric center. This singularity can be locally or globally naked in accordance with the initial rest-mass density configuration. The solution of the Einstein equations describing such a situation is known as the LTB space-time. The line element is given by

$$ds^2 = -dt^2 + \frac{(\partial_r R)_t^2}{1 + f(r)} dr^2 + R^2 d\Omega^2, \quad (2.1)$$

where $d\Omega^2$ is the line element of an unit 2-sphere. The stress-energy tensor of the dust fluid is given by

$$T_{ab} = \bar{\rho} \bar{u}_a \bar{u}_b, \quad (2.2)$$

where $\bar{\rho}$ is the rest-mass density and \bar{u}_a is the 4-velocity of the dust fluid element. In the coordinate system (2.1), the components of the 4-velocity \bar{u}^μ is given by

$$\bar{u}^\mu = (1, 0, 0, 0). \quad (2.3)$$

Einstein equations and the equation of motion for the dust fluid lead to the equations for the areal radius R and rest-mass density $\bar{\rho}$ as

$$(\partial_t R)_r^2 = f(r) + \frac{F(r)}{R}, \quad (2.4)$$

$$F(r) = 8\pi \int_0^r \bar{\rho} (\partial_r R)_t R^2 dr, \quad (2.5)$$

where $f(r)$ and $F(r)$ are arbitrary functions. Eq.(2.4) might be regarded as an energy equation of the dust fluid element at r . From this point of view, the function $f(r)$ corresponds to the specific energy of the dust fluid element and the function $F(r)$ can be regarded as the gravitational mass function. The solution is completely fixed by choosing the specific energy $f(r)$ and initial rest-mass density profile $\bar{\rho}(0, r)$, or equivalently the mass function $F(r)$. The shell focusing naked singularity is formed only at $r = 0$.

For simplicity, hereafter we will focus on the marginally bound case $f(r) = 0$. Since our interest is on the behavior of the space-time near the central singularity, this restriction might not lose generality of the conclusion. The solution of Eq.(2.4) is given by

$$R = \left(\frac{9F}{4} \right)^{\frac{1}{3}} [t_R(r) - t]^{\frac{2}{3}}, \quad (2.6)$$

where $t_R(r)$ is an arbitrary function which corresponds to the moment of the singularity formation. We choose the time of singularity formation as

$$t_R(r) = \frac{r^{3/2}}{3} \sqrt{\frac{4}{F}}, \quad (2.7)$$

so that R agrees with r at $t = 0$.

In the spherically symmetric space-time, we can naturally introduce a “gravitational potential” Φ_G defined by

$$\Phi_G \equiv \frac{F}{R}. \quad (2.8)$$

As Hayward discussed, the gravitational potential Φ_G is deeply related to the formation of trapped region and hence gives a measure of the strength of the gravitational field [31]. To see the behavior of the gravitational potential Φ_G and the velocity $(\partial_t R)_r$ of the dust fluid element, we adopt the following initial density configuration for $\bar{\rho}$

$$\bar{\rho}(0, r) = \frac{1}{8\pi r^2} \frac{dF}{dr} = \frac{1}{6\pi} \left\{ 1 + \exp\left(-\frac{r_1}{2r_2}\right) \right\} \left\{ 1 + \exp\left(\frac{r^2 - r_1^2}{2r_1 r_2}\right) \right\}^{-1}, \quad (2.9)$$

where r_1 and r_2 are positive constants. Since a sufficient condition for the nakedness of the central shell focusing singularity is $\partial_r^2 \rho(0, r) < 0$ [7,8], the above initial density distribution necessarily leads to the naked singularity at the symmetric center $r = 0$. Here note that the moment of the central shell focusing singularity is $t = 1$ by the above initial density profile. The core radius of the above configuration is given by

$$r_{\text{core}} = r_1 + \frac{1}{2}r_2. \quad (2.10)$$

If we set appropriate r_1 and r_2 , the space-time is globally naked singular. In Fig.1, we depict the gravitational potential Φ_G with $r_1 = 2 \times 10^{-2}$ and $r_2 = 10^{-2}$. We see that the gravitational potential Φ_G is much smaller than unity even at the moment of the central shell focusing naked singularity formation. Note that from Eq.(2.4), $|(\partial_t R)_r|$ is also much smaller than unity. Hence in this example, the Newtonian approximation scheme seems to be available and in reality it is true as will be shown in the next section.

III. NEWTONIAN APPROXIMATION

In this section, we consider gravitational collapse of a spherically symmetric dust fluid in the framework of the Newtonian approximation and show that the Newtonian approximation is valid even at the moment of the central shell focusing naked singularity formation if the initial condition is appropriately set up as in the case of the example in the previous section.

A. Eulerian Coordinate

In the Newtonian approximation, the maximal time slicing condition and Eulerian coordinate (for example, the minimal distortion gauge condition) are usually adopted. The line element is expressed in the following form

$$ds_E^2 = -(1 + 2\Phi_N) dT^2 + dR^2 + R^2 d\Omega^2, \quad (3.1)$$

where Φ_N is Newtonian gravitational potential and we have adopted the spherical-polar coordinate system as a spatial coordinates. The equations for the spherically symmetric dust fluid and Newtonian gravitational potential Φ_N are given by

$$\partial_T \bar{\rho} + \frac{1}{R^2} \partial_R (R^2 \bar{\rho} V) = 0, \quad (3.2)$$

$$\partial_T V + V \partial_R V = -\partial_R \Phi_N, \quad (3.3)$$

$$\frac{1}{R^2} \partial_R (R^2 \partial_R \Phi_N) = 4\pi \bar{\rho}, \quad (3.4)$$

where V is the velocity of the dust fluid element. The assumptions in the Newtonian approximation are

$$|V| \ll 1, \quad \text{and} \quad |\Phi_N| \ll 1, \quad (3.5)$$

and further

$$|\partial_T V| \ll |\partial_R V|, \quad |\partial_T \Phi_N| \ll |\partial_R \Phi_N| \quad \text{and} \quad |\partial_T \bar{\rho}| \ll |\partial_R \bar{\rho}|. \quad (3.6)$$

B. Lagrangian Coordinate

For the purpose to follow the motion of a dust sphere, the Lagrangian coordinate is more suitable than the Eulerian one. The transformation matrix between the Eulerian and Lagrangian coordinate systems is given by

$$dT = d\tau, \quad (3.7)$$

$$dR = \dot{R} d\tau + R' dx, \quad (3.8)$$

where regarding τ and x as the independent variables, a dot means a partial derivative with respect to τ while a prime denotes a partial derivative with respect to x . Then the line element in the Lagrangian coordinate system is obtained as

$$ds_L^2 = - \left(1 + 2\Phi_N - \dot{R}^2 \right) d\tau^2 + 2\dot{R}R' d\tau dx + R'^2 dx^2 + R^2 d\Omega^2. \quad (3.9)$$

Equations for the dust fluid and Newtonian gravitational potential are given by

$$F(x) = 8\pi \int_0^x \bar{\rho} R' R^2 dx, \quad (3.10)$$

$$V^2 = \dot{R}^2 = f(x) + \frac{F(x)}{R}, \quad (3.11)$$

$$\Phi'_N = \frac{R'}{2R^2} F(x), \quad (3.12)$$

where $f(x)$ and $F(x)$ are regarded as arbitrary functions. Since the equation for the areal radius R is the same as that of the LTB space-time, its solution for the marginally bound collapse $f(x) = 0$ is given by the same functional form as Eq.(2.6),

$$R = \left(\frac{9F}{4} \right)^{\frac{1}{3}} [\tau_R(x) - \tau]^{\frac{2}{3}}, \quad (3.13)$$

where $\tau_R(x)$ is an arbitrary function which determines the moment of singularity formation.

Here we consider the Newtonian approximation of the example given in the previous section. Hence we choose the moment of the singularity formation as

$$\tau_R(x) = \frac{x^{3/2}}{3} \sqrt{\frac{4}{F}} \quad (3.14)$$

so that R agrees with x at $\tau = 0$. As for the initial density configuration, we adopt the same functional form as Eq.(2.9),

$$\bar{\rho}(0, x) = \frac{F'}{8\pi x^2} = \frac{1}{6\pi} \left\{ 1 + \exp\left(-\frac{x_1}{2x_2}\right) \right\} \left\{ 1 + \exp\left(\frac{x^2 - x_1^2}{2x_1 x_2}\right) \right\}^{-1}, \quad (3.15)$$

where x_1 and x_2 are positive constants. The above choice guarantees the regularity of all the variables before the singularity formation and that the central shell focusing singularity is formed at $\tau = 1$.

Imposing a boundary condition $\Phi_N \rightarrow 0$ for $x \rightarrow \infty$, the solution of Eq.(3.12) is formally expressed as

$$\Phi_N = \Phi_{N1}(\tau, x) + \Phi_{N2}(\tau), \quad (3.16)$$

where

$$\Phi_{N1}(\tau, x) \equiv \int_0^x \frac{R'}{2R^2} F dx, \quad (3.17)$$

$$\Phi_{N2}(\tau) \equiv - \int_0^\infty \frac{R'}{2R^2} F dx = -\frac{1}{2} \int_0^\infty \frac{F'}{R} dx. \quad (3.18)$$

The behavior of F/R is the same as that of Φ_G as shown in Fig.1. On the other hand, the Newtonian gravitational potential Φ_N of $x_1 = 2 \times 10^{-2}$ and $x_2 = 10^{-2}$ is depicted in Fig.2(a). From these figures, we find that the condition (3.5) is satisfied even at the moment of the central shell focusing naked singularity formation. Here it is worthwhile to note that the right hand side of Eq.(3.12) at $x = 0$ diverges at the moment of the central shell focusing naked singularity formation,

$$\Phi'_N \longrightarrow \frac{14}{27\tau_{R(1)}^{2/3}} x^{-1/3} \quad \text{for } x \longrightarrow 0 \quad \text{at } \tau = 1, \quad (3.19)$$

where

$$\tau_{R(1)} \equiv \frac{1}{2} \frac{d^2 \tau_R(x)}{dx^2} \Big|_{x=0}. \quad (3.20)$$

However since the power index of x is larger than -1 , Φ_N itself is finite at $x = 0$ even at the moment of the central shell focusing singularity formation $\tau = 1$.

In order that the Newtonian approximation is successful, temporal derivatives of all the quantities should always smaller than the radial derivatives of those. Here we shall focus on the neighborhood of the central shell focusing naked singularity only. For this purpose, we introduce a new variable w defined by

$$w \equiv \delta\tau^{-1/2}x. \quad (3.21)$$

where $\delta\tau \equiv (1 - \tau)/\tau_{R(1)}$. Then we consider a limit $\tau \rightarrow 1$ with fixed w . It should be noted that x also goes to zero by this limiting procedure. The mass function F , rest-mass density $\bar{\rho}$ and areal radius R behave as

$$F \longrightarrow \frac{4}{9}w^3\delta\tau^{3/2}, \quad (3.22)$$

$$\bar{\rho} \longrightarrow \frac{1}{2\pi}\tau_{R(1)}^{-2}(3 + 7w^2)^{-1}(1 + w^2)^{-1}\delta\tau^{-2}, \quad (3.23)$$

$$R \longrightarrow \tau_{R(1)}^{2/3}w(1 + w^2)^{2/3}\delta\tau^{7/6}. \quad (3.24)$$

All these variables are proportional to the power of $\delta\tau$ and the coefficients of those are functions of w . It is easy to see that their derivatives with respect to τ or x also take the same functional structure with respect to $\delta\tau$ and w . Thus the x -dependent part Φ_{N1} of the Newtonian gravitational potential will also behave in the manner

$$\Phi_{N1} \longrightarrow \phi_{N1}(w)\delta\tau^i, \quad (3.25)$$

where i is a constant and ϕ_N is a function of w . Substituting the above equation into Eq.(3.12) and using the asymptotic behavior (3.22) and (3.24), we obtain

$$\frac{d\phi_{N1}(w)}{dw}\delta\tau^{i-1/2} = \frac{2w(3 + 7w^2)}{27\tau_{R(1)}^{2/3}(1 + w^2)^{5/3}}\delta\tau^{-1/6}. \quad (3.26)$$

In order that the dependence of both sides in the above equation on $\delta\tau$ agrees with each other, i should be equal to $1/3$. Integration of Eq.(3.26) leads to

$$\phi_{N1}(w) = \frac{1}{9\tau_{R(1)}^{2/3}(1 + w^2)^{2/3}} \left\{ 7(1 + w^2) - 9(1 + w^2)^{2/3} + 2 \right\}. \quad (3.27)$$

In order to see the asymptotic dependence of $\Phi_{N2}(\tau)$ on τ , we differentiate Eq.(3.18) to obtain

$$\dot{\Phi}_{N2} = -\frac{1}{2} \int_0^\infty \frac{F'}{R^2} \sqrt{\frac{F}{R}} dx. \quad (3.28)$$

The integrand in the right hand side of the above equation behaves near the origin at the moment of the central shell focusing singularity formation as

$$\frac{F'}{R^2} \sqrt{\frac{F}{R}} \longrightarrow \frac{8}{9\tau_{R(1)}^{5/3}} x^{-7/3} \quad \text{for } x \longrightarrow 0 \quad \text{at } \tau = 1. \quad (3.29)$$

Therefore, the integral in Eq.(3.28) does not have finite value at $\tau = 1$. Since as shown in the above, this divergence comes from the irregularity of the integrand at the origin $x = 0$, we shall estimate the contribution near the origin to the integral in Eq.(3.28). We again consider the limit of $\delta\tau \rightarrow 0$ with fixed w and obtain

$$\int_0^\infty \frac{F'}{R^2} \sqrt{\frac{F}{R}} dx \longrightarrow \frac{8}{9\tau_{R(1)}^{5/3}} \delta\tau^{-2/3} \int_0^\infty \frac{wdw}{(1 + w^2)^{5/3}} = \frac{2}{3\tau_{R(1)}^{5/3}} \delta\tau^{-2/3}. \quad (3.30)$$

Substituting the above equation into Eq.(3.28) and integrating it with respect to τ , we obtain

$$\Phi_{N2} \longrightarrow \frac{\delta\tau^{1/3}}{\tau_{R(1)}^{2/3}} + \Phi_{N2}(1). \quad (3.31)$$

As a result, in the limit of $\delta\tau \rightarrow 0$ with fixed w , Φ_N is expressed in the form

$$\Phi_N \longrightarrow \frac{9 + 7w^2}{9\tau_{R(1)}^{2/3}(1 + w^2)^{2/3}} \delta\tau^{1/3} + \Phi_{N2}(1). \quad (3.32)$$

We depict numerically obtained Φ_N together with the above asymptotic form in Fig.2(b). The asymptotic estimate agrees with the numerical result quite well.

Now we have known that in the limit of $\delta\tau \rightarrow 0$ with fixed w , all the variables behave as

$$Z(\tau, x) \longrightarrow z(w)\delta\tau^j + \text{constant}, \quad (3.33)$$

where $z(w)$ is some function of w and j is a constant. The derivatives of Z with respect to T and R are expressed by using its derivatives with respect to τ and x as

$$(\partial_T Z)_R = (\partial_T \tau)_R \dot{Z} + (\partial_T x)_R Z', \quad (3.34)$$

$$(\partial_R Z)_T = (\partial_R \tau)_T \dot{Z} + (\partial_R x)_T Z'. \quad (3.35)$$

From Eqs.(3.7) and (3.8), we find

$$(\partial_T \tau)_R = 1, \quad (\partial_R \tau)_T = 0, \quad (\partial_T x)_R = -\frac{\dot{R}}{R'}, \quad \text{and} \quad (\partial_R x)_T = \frac{1}{R'}. \quad (3.36)$$

Then the following relation is derived,

$$\frac{(\partial_T Z)_R}{(\partial_R Z)_T} = R' \frac{\dot{Z}}{Z'} - \dot{R}. \quad (3.37)$$

Inserting Eq.(3.33) into the above equation, we obtain

$$\frac{(\partial_T Z)_R}{(\partial_R Z)_T} \longrightarrow \frac{1}{3\tau_{R(1)}^{1/3}(1 + w^2)^{1/3}} \left\{ \frac{1}{2}w(1 + 7w^2) - jz(3 + 7w^2) \left(\frac{dz}{dw} \right)^{-1} \right\} \delta\tau^{\frac{1}{6}}. \quad (3.38)$$

The above equation means that in the limit of $\delta\tau \rightarrow 0$ with fixed w , the following inequality holds

$$|(\partial_T Z)_R| \ll |(\partial_R Z)_T|. \quad (3.39)$$

Therefore, the order counting of the Newtonian approximation is guaranteed even in the neighborhood of the central naked singularity.

Here it is worthy to notice that in the limit of $\delta\tau \rightarrow 0$ with fixed w , $|\dot{Z}|$ is much larger than $|Z'|$ because of

$$\frac{\dot{Z}}{Z'} \longrightarrow \frac{1}{\tau_{R(1)}} \left(\frac{1}{2}w - jz \frac{dw}{dz} \right) \delta\tau^{-1/2} \longrightarrow \infty. \quad (3.40)$$

Hence the vicinity of the central shell focusing naked singularity is not Newtonian situation in ordinary sense. In reality, the present authors have shown that the violent quantum particle creation occurs in such a situation [28,29]. This means that the formation of the central shell focusing singularity is a highly relativistic phenomenon even though it is well described by the Newtonian approximation in the Eulerian coordinate system.

C. Synchronous-Comoving Coordinate

In the LTB solution, the SC coordinate system is adopted. We should note that the SC coordinate system is different from the Lagrangian one. We consider the following coordinate transformation

$$dt = \left\{ 1 + \Phi_N - \frac{1}{2}(\partial_\tau R)_x^2 \right\} d\tau - (\partial_\tau R)_x (\partial_x R)_\tau dx, \quad (3.41)$$

$$dr = dx. \quad (3.42)$$

Assuming Eq.(3.5), derivatives of the areal radius R with respect to the Lagrangian time coordinate τ and the radial coordinate x are written as

$$\dot{R} = (\partial_\tau t)_x (\partial_t R)_r + (\partial_\tau r)_x (\partial_r R)_t = \{1 + \Phi_N - (\partial_\tau R)_x^2\} (\partial_t R)_x \sim (\partial_x R)_\tau, \quad (3.43)$$

$$R' = (\partial_x t)_\tau (\partial_t R)_r + (\partial_x r)_\tau (\partial_r R)_t = (\partial_r R)_t - (\partial_\tau R)_x (\partial_x R)_\tau (\partial_t R)_r \sim (\partial_r R)_t. \quad (3.44)$$

Hence the line element in the new coordinate system t, r up to the lowest order in the sense of Eq.(3.5) is written as

$$ds_{\text{SC}}^2 = -dt^2 + (\partial_r R)_t^2 dr^2 + R^2 d\Omega^2. \quad (3.45)$$

From the above equation, we find that the coordinate transformation (3.41) and (3.42) leads to the SC coordinate system. Especially, the above line element is completely the same as the relativistic one in the marginally bound case. Further we obtain the equations of the lowest order in the SC coordinate system are given in completely the same form as that in the relativistic one:

$$(\partial_t R)_r^2 = f(r) + \frac{F(r)}{R}, \quad (3.46)$$

$$F(r) = 8\pi \int_0^r \bar{\rho} (\partial_r R)_t R^2 dr. \quad (3.47)$$

It is worthwhile to note that in the SC coordinate system, the Newtonian gravitational potential Φ_N does not appear.

IV. BASIC EQUATIONS OF EVEN MODE PERTURBATIONS

We consider non-spherical linear perturbations in the system of the spherically symmetric dust ball described in the previous section. First, we consider perturbations in the Eulerian coordinate system. The line element is written as

$$ds_{\text{E}}^2 = -(1 + 2\Phi_N + 2\delta\Phi_N) dT^2 + dR^2 + R^2 d\Omega^2, \quad (4.1)$$

where $\delta\Phi_N$ is a perturbation of the Newtonian gravitational potential. Using the transformation matrix (3.7) and (3.8), we obtain the perturbed line element in the background Lagrangian coordinate system as

$$ds_{\text{L}}^2 = -\left(1 + 2\Phi_N + 2\delta\Phi_N - \dot{R}^2\right) d\tau^2 + 2\dot{R}R' d\tau dx + R'^2 dx^2 + R^2 d\Omega^2. \quad (4.2)$$

Hereafter we discuss the behavior of perturbations in this coordinate system. The density ρ and 4-velocity u^μ are written in the form

$$\rho = \bar{\rho}(1 + \delta_\rho), \quad (4.3)$$

$$u^\mu = \bar{u}^\mu + \delta u^\mu. \quad (4.4)$$

By definition of the Lagrangian coordinate system, the components of the background 4-velocity is given by

$$(\bar{u}^\mu) = (\bar{u}^0, 0, 0, 0). \quad (4.5)$$

From the normalization of the 4-velocity, we find

$$\delta u^0 = -\delta\Phi_N + \dot{R}R'\delta u^1. \quad (4.6)$$

The order-counting with respect to the expansion parameter ε of the Newtonian approximation is given by

$$\delta u^0 = O(\varepsilon^2), \quad \delta u^\ell = O(\varepsilon), \quad \delta_\rho = O(\varepsilon^0) \quad \text{and} \quad \delta\Phi_N = O(\varepsilon^2). \quad (4.7)$$

Then the equations for the perturbations are given by

$$\partial_\tau \delta_\rho + \frac{1}{\bar{\rho}\sqrt{\bar{\gamma}}} \partial_\ell (\bar{\rho}\sqrt{\bar{\gamma}} \delta u^\ell) = 0, \quad (4.8)$$

$$\partial_\tau \delta u_\ell + \partial_\ell \delta \Phi_N = 0, \quad (4.9)$$

$$\frac{1}{\sqrt{\bar{\gamma}}} \partial_\ell (\sqrt{\bar{\gamma}} \bar{\gamma}^{\ell m} \partial_m \delta \Phi_N) - 4\pi \bar{\rho} \delta_\rho = 0, \quad (4.10)$$

where

$$\sqrt{\bar{\gamma}} \equiv R' R^2 \sin \theta, \quad (4.11)$$

and $\bar{\gamma}^{\ell m}$ is a contravariant component of the background 3-metric.

Here we focus on the axisymmetric even mode of perturbations. Hence the perturbations are expressed in the form

$$\delta_\rho = \sum_l \Delta_{\rho(l)}(\tau, x) P_l(\cos \theta), \quad (4.12)$$

$$\delta \Phi_N = \sum_l \Delta_{\Phi(l)}(\tau, x) P_l(\cos \theta), \quad (4.13)$$

$$\delta u_1 = \sum_l U_{x(l)}(\tau, x) P_l(\cos \theta), \quad (4.14)$$

$$\delta u_2 = \sum_l U_{\theta(l)}(\tau, x) \frac{d}{d\theta} P_l(\cos \theta), \quad (4.15)$$

$$\delta u_3 = 0. \quad (4.16)$$

From Eqs.(4.8), (4.9) and (4.10), we obtain

$$\Delta_{\rho(l)} + \frac{1}{F'} \left(\frac{F'}{R'^2} U_{x(l)} \right)' - l(l+1) \frac{U_{\theta(l)}}{R^2} = 0, \quad (4.17)$$

$$\dot{U}_{x(l)} + \Delta'_{\Phi(l)} = 0, \quad (4.18)$$

$$\dot{U}_{\theta(l)} + \Delta_{\Phi(l)} = 0, \quad (4.19)$$

$$\frac{1}{R' R^2} \left(\frac{R^2}{R'} \Delta'_{\Phi(l)} \right)' - l(l+1) \frac{\Delta_{\Phi(l)}}{R^2} - 4\pi \bar{\rho} \Delta_{\rho(l)} = 0, \quad (4.20)$$

Comparing the basic equations for the relativistic perturbations of $l = 2$ in Ref. [24] to the above equations, we find the correspondence between the Newtonian and relativistic variables; $\Delta_{\Phi(2)} = -2K$, $U_{x(2)} = -V_1$ and $U_{\theta(2)} = -V_2$.

V. MASS-QUADRUPOLE FORMULA

Hereafter we focus on the quadrupole mode $l = 2$ and therefore omit the subscript (l) to specify the multi-pole component of the perturbation variable. The mass-quadrupole moment $Q_{\ell m}$ is given by

$$Q_{\ell m} \equiv \int \rho \left(X_\ell X_m - \frac{1}{3} R^2 \delta_{\ell m} \right) d^3 X = \frac{4\pi}{15} Q(T) \text{diag}[-1, -1, 2], \quad (5.1)$$

where

$$Q(T) \equiv \int_0^\infty \bar{\rho} \Delta_\rho R^4 dR. \quad (5.2)$$

For a function $g(\tau, x)$ with sufficiently rapid fall off for $x \rightarrow \infty$, we find that

$$\frac{d}{dT} \int_0^\infty g dR = \int_0^\infty (\partial_T g)_R dR = \int_0^\infty \left(\dot{g} - \frac{\dot{R}}{R'} g' \right) R' dx \quad (5.3)$$

$$= \int_0^\infty (R' \dot{g} + \dot{R}' g) dx - [\dot{R} g]_0^\infty = \int_0^\infty \partial_\tau (R' g) dx. \quad (5.4)$$

Using the above formula, we obtain

$$\frac{d^m Q}{dT^m} = \int_0^\infty \frac{\partial^m}{\partial \tau^m} (\bar{\rho} \Delta_\rho R' R^4) dx = \frac{1}{8\pi} \int_0^\infty F' \frac{\partial^m}{\partial \tau^m} (\Delta_\rho R^2) dx. \quad (5.5)$$

The power L_{GW} carried by the gravitational radiation at the future null infinity $T + R \rightarrow \infty$ is given by

$$L_{\text{GW}} = \frac{32\pi^2}{375} \left(\frac{d^3 Q(u)}{du^3} \right)^2, \quad (5.6)$$

where $u \equiv T - R$ is the retarded time. The Weyl scalar Ψ_4 carried by outgoing gravitational waves at the future null infinity is estimated as

$$\Psi_4 = -C_{abcd} n^a \bar{m}^b n^c \bar{m}^d = -\frac{3\pi}{5} \frac{d^4 Q(u)}{du^4} \sin^2 \theta, \quad (5.7)$$

where C_{abcd} is the Weyl tensor, and n^a and \bar{m}^a are two of the null tetrad basis whose components in the spherical polar coordinate are given by

$$(n_\mu) = \frac{1}{\sqrt{2}}(1, -1, 0, 0), \quad (5.8)$$

$$(\bar{m}_\mu) = \frac{1}{\sqrt{2}}(0, 0, R, -iR \sin \theta). \quad (5.9)$$

It should be noted that the power L_{GW} is proportional to the square of the 3rd-order derivative of $Q(u)$ while the Weyl scalar Ψ_4 is proportional to the 4th-order derivatives of $Q(u)$.

VI. NUMERICAL SIMULATION

In this section, we explain the procedure to numerically integrate the system of partial differential equations for the quadrupole perturbation variables and show the time evolution of the mass-quadrupole moment.

A. Basic Equation

We assume that all the perturbation variables are regular before the central shell focusing singularity formation and hence are written in the form of the Taylor series as

$$\Delta_\rho = x^2 \Delta_\rho^* = x^2 \sum_{n=0}^\infty \Delta_{\rho(n)}^* x^{2n}, \quad (6.1)$$

$$U_x = x U_x^* = x \sum_{n=0}^\infty U_{x(n)}^* x^{2n}, \quad (6.2)$$

$$U_\theta = x^2 U_\theta^* = x^2 \sum_{n=0}^\infty U_{\theta(n)}^* x^{2n}, \quad (6.3)$$

$$\Delta_\Phi = x^2 \Delta_\Phi^* = x^2 \sum_{n=0}^\infty \Delta_{\Phi(n)}^* x^{2n}. \quad (6.4)$$

In the numerical calculation, we focus on the above asterisked variables rather than the original variables.

To obtain the solution of Eq.(4.20), we introduce a variable \mathcal{Q} defined by

$$\Delta_\Phi = \frac{\mathcal{Q}(\tau, x)}{R^3}. \quad (6.5)$$

Substituting the above form of Δ_Φ into Eq.(4.20), we obtain the equation for \mathcal{Q} as

$$\left(\frac{1}{R'R^4}\mathcal{Q}'\right)' = \frac{F'\Delta_\rho}{2R^3}. \quad (6.6)$$

Integrating the above equation, we obtain

$$\mathcal{Q}' = -\frac{1}{2}R'R^4 \int_x^\infty dx_1 \frac{F'(x_1)}{R^3(\tau, x_1)} \Delta_\rho(\tau, x_1), \quad (6.7)$$

where we have chosen the integration constant so that \mathcal{Q}' is finite for $x \rightarrow \infty$. Further integration leads to

$$\begin{aligned} \mathcal{Q}(\tau, x) &= -\frac{1}{2} \int_0^x dx_1 R'(\tau, x_1) R^4(\tau, x_1) \int_{x_1}^\infty dx_2 \frac{F'(x_2)}{R^3(\tau, x_2)} \Delta_\rho(\tau, x_2) \\ &= -\frac{1}{2} \int_0^x dx_1 R'(\tau, x_1) R^4(\tau, x_1) \int_x^\infty dx_2 \frac{F'(x_2)}{R^3(\tau, x_2)} \Delta_\rho(\tau, x_2) \\ &\quad - \frac{1}{2} \int_0^x dx_2 \frac{F'(x_2)}{R^3(\tau, x_2)} \Delta_\rho(\tau, x_2) \int_0^{x_2} dx_1 R'(\tau, x_1) R^4(\tau, x_1) \\ &= -\frac{1}{10} \{R^5 \mathcal{A}(\tau, x) + x^7 \mathcal{B}(\tau, x)\}. \end{aligned} \quad (6.8)$$

where

$$\mathcal{A}(\tau, x) \equiv \int_x^\infty dx_1 \frac{F'(x_1)}{R^3(\tau, x_1)} \Delta_\rho(\tau, x_1), \quad (6.9)$$

$$\mathcal{B}(\tau, x) \equiv \frac{1}{x^7} \int_0^x dx_1 F'(x_1) \Delta_\rho(\tau, x_1) R^2(\tau, x_1), \quad (6.10)$$

and we have chosen the integration constant so that \mathcal{Q} vanishes at the origin, $x = 0$. Hence Δ_Φ^* is written as

$$\Delta_\Phi^* = -\frac{1}{10} \left\{ \left(\frac{R}{x}\right)^2 \mathcal{A} + x^2 \left(\frac{x}{R}\right)^3 \mathcal{B} \right\}. \quad (6.11)$$

For the numerical calculation, we rewrite the basic equations (4.17)–(4.19) for the perturbation variables. Differentiating the conservation law (4.17) with respect to time τ and then using Eqs.(4.17)–(4.19), we obtain a second order differential equation with respect to τ for Δ_ρ^* as

$$\frac{\partial V_\rho^*}{\partial \tau} = -2 \frac{\dot{R}'}{R'} V_\rho^* + \frac{F'}{2R'R^2} \Delta_\rho^* + \frac{2}{xR'^2} \left(\frac{\dot{R}'}{R'}\right)' U_x^* - \frac{12}{R^2} \left(\frac{\dot{R}}{R} - \frac{\dot{R}'}{R'}\right) U_\theta^* + \frac{R^2}{xF'R'} \left(\frac{F'}{R'R^2}\right)' D_\Phi^*, \quad (6.12)$$

$$\frac{\partial \Delta_\rho^*}{\partial \tau} = V_\rho^*, \quad (6.13)$$

$$(6.14)$$

where

$$D_\Phi^* \equiv \frac{1}{x} (x^2 \Delta_\Phi^*)' = -\frac{R'}{10} \left\{ 2 \left(\frac{R}{x}\right) \mathcal{A} - 3x^2 \left(\frac{x}{R}\right)^4 \mathcal{B} \right\}. \quad (6.15)$$

The equations for U_x^* and U_θ^* are written as

$$\frac{\partial U_x^*}{\partial \tau} = -D_\Phi^*, \quad (6.16)$$

$$\frac{\partial U_\theta^*}{\partial \tau} = -\Delta_\Phi^*. \quad (6.17)$$

Eqs.(6.11)–(6.17) constitute a closed system of equations, which is solved numerically.

The background solution is given by (3.13), (3.14) and (3.15). The parameters x_1 and x_2 in $\bar{\rho}(0, x)$ are chosen to be $x_1 = 2 \times 10^{-2}$ and $x_2 = 10^{-2}$, respectively. Then the core radius x_{core} of the background rest-mass density distribution becomes

$$x_{\text{core}} = x_1 + \frac{1}{2}x_2 = 1.25 \times 10^{-2}. \quad (6.18)$$

We start the numerical integration at $\tau = 0$. The initial data of the density perturbation Δ_ρ^* is set up in the form

$$\Delta_\rho^*(0, x) = \exp \left\{ -\frac{1}{2} \left(\frac{x}{\sigma_\rho x_c} \right)^2 \right\}. \quad (6.19)$$

where σ_ρ is a positive constant smaller than unity. We set $\sigma_\rho = 0.5$.

From Eqs.(4.18) and (4.19), we find

$$\partial_\tau (U_x - U'_\theta) = 0. \quad (6.20)$$

Hence U_x is written in the form

$$U_x = U'_\theta + C_x(x), \quad (6.21)$$

where C_x is an arbitrary function. As for the initial data, we set $U_\theta = 0$ and

$$C_x = c_x x^3 \exp \left\{ -\frac{1}{2} \left(\frac{x}{\sigma_x x_c} \right)^2 \right\}, \quad (6.22)$$

where σ_x is a positive constant smaller than unity and c_x is also a constant. From Eq.(4.17), the initial data for V_ρ^* should be

$$V_\rho^*(0, x) = -\frac{1}{x^2 F'} (F' C_x)'. \quad (6.23)$$

C. Numerical Scheme

The temporal integration of Eqs.(6.12)–(6.17) is performed by the second order Runge-Kutta method. In order to obtain Δ_Φ^* and D_Φ^* , we numerically integrate Eqs.(6.9) and (6.10) also by the second order Runge-Kutta method and then substitute the results into Eqs.(6.11) and (6.15).

The number of spatial grid points is 5×10^4 and the outermost grid point corresponds to $x = 10x_c$. Since we numerically integrate the second order differential equation with respect to τ for the density perturbation Δ_ρ^* , the conservation law (4.17) is not trivially satisfied by the numerical error. Hence we use Eq.(4.17) as a check of accuracy of the numerical integration. We define the error function \mathcal{E} as

$$\mathcal{E} \equiv 4 \left| V_\rho^* + \frac{U_x^*}{x R'^2} + \frac{U_x^*}{x^2 F'} \left(\frac{x F'}{R'^2} \right)' - \frac{6}{R^2} U_\theta^* \right| \left[|V_\rho^*| + \left| \frac{U_x^*}{x R'^2} \right| + \left| \frac{U_x^*}{x^2 F'} \left(\frac{x F'}{R'^2} \right)' \right| + \left| \frac{6}{R^2} U_\theta^* \right| \right]^{-1}. \quad (6.24)$$

We perform the numerical integration until $1 - \tau = 2 \times 10^{-4}$. The function \mathcal{E} in $x \leq x_c$ is less than 10^{-3} . Hence the numerical integration is almost consistently performed near the origin and hence we can observe the asymptotic behavior of the contribution near the central shell focusing singularity to the mass-quadrupole moment in the limit of $\tau \rightarrow 1$.

D. Behavior of the Mass-Quadrupole Moment

In Fig3, we show $d^2 Q/dT^2$, $d^3 Q/dT^3$ and $d^4 Q/dT^4$. The numerical integration was performed from $1 - \tau = 1$ to $1 - \tau = 2 \times 10^{-4}$. From this figure, we find that those variables do not show power-law behavior with respect to $1 - \tau$ but rather their behavior is oscillatory and growing. At this stage, the mass-quadrupole moment is determined mainly by the motion of dust fluid in the outside region and the contribution in the neighborhood of the central shell focusing singularity is still negligible. However, the contribution near the origin will be dominant in the limit $\tau \rightarrow 1$ as will be shown in the next section.

In order to get information of the asymptotic behavior of the mass-quadrupole moment, we should carefully examine the asymptotic behavior of the perturbation variables near the origin. For this purpose, we introduce w defined in Eq.(3.21) and then consider the limit $\tau \rightarrow 1$ with fixed w . Since all the background variables appearing in the equations of the perturbations are proportional to the power of $\delta\tau$ and the coefficients of those are the functions of w as Eqs.(3.22)–(3.24) and (3.32), we expect that the perturbation variables also behave in the same manner as the background variables and hence we assume

$$\Delta_\rho^* = \delta_\rho^*(w)\delta\tau^{-p}, \quad (7.1)$$

$$U_x^* = \frac{1}{x}\partial_x(x^2 U_\theta^*) = \tau_{R(1)}^{1/3} \left(w \frac{du_\theta^*}{dw} + 2u_\theta^* \right) \delta\tau^{-q}, \quad (7.2)$$

$$U_\theta^* = \tau_{R(1)}^{1/3} u_\theta^*(w)\delta\tau^{-q}, \quad (7.3)$$

$$\Delta_\Phi^* = \tau_{R(1)}^{-2/3} \delta_\Phi^*(w)\delta\tau^{-r}, \quad (7.4)$$

where we have assumed that the contribution of C_x to U_x^* is negligible in the limit of $\tau \rightarrow 1$. In Fig.4, we depict the numerical results for the asterisked variables at the origin as functions of $1 - \tau$ in the case of $C_x = 0$. From this figure, we can easily find that the hatted variables show the power-low behavior and grow monotonically. The power indices are estimated as

$$p = 1.70, \quad q = 0.38 \quad \text{and} \quad r = 1.37. \quad (7.5)$$

Due to this growing behavior, in reality, the contribution of C_x to U_x^* becomes negligible in the limit $\tau \rightarrow 1$. Although we do not show the case of $C_x \neq 0$, we have confirmed that the behavior of the asterisked variables in the case of $C_x \neq 0$ is almost identical to the case of $C_x = 0$ in the limit $\tau \rightarrow 1$.

Next we depict the following normalized perturbation variables with respect to w for $x < 0.05x_{\text{core}}$ at various time steps for the time interval $2.0 \times 10^{-4} \leq 1 - \tau \leq 6.6 \times 10^{-3}$ in Figs.5, 6 and 7;

$$\Delta_\rho^\dagger \equiv \Delta_\rho^*(\tau, x)/\Delta_\rho^*(\tau, 0), \quad (7.6)$$

$$U_\theta^\dagger \equiv U_\theta^*(\tau, x)/U_\theta^*(\tau, 0), \quad (7.7)$$

$$\Delta_\Phi^\dagger \equiv \Delta_\Phi^*(\tau, x)/\Delta_\Phi^*(\tau, 0). \quad (7.8)$$

Note that $\Delta_\rho^*(\tau, 0)$ at $1 - \tau = 2 \times 10^{-4}$ becomes 381 times larger than that at $1 - \tau = 6.6 \times 10^{-3}$. As expected, the spatial configuration of these variables with respect to w are almost time independent. Hence the assumptions (7.1)–(7.4) are justified by the numerical calculation.

Now, by virtue of our knowledge about the asymptotic forms (7.1)–(7.4), more rigorous discussion about the evolution of the mass-quadrupole moment is possible. Substituting Eqs.(7.1)–(7.4) into Eqs.(4.17)–(4.20), and using the asymptotic behavior of the background variables (3.22)–(3.24), we obtain

$$\left(w \frac{d\delta_\rho^*}{dw} + 2p\delta_\rho^* \right) \delta\tau^{-p-1} + \left[\frac{18}{w^4} \frac{d}{dw} \left\{ \frac{w^2(1+w^2)^{2/3}}{(3+7w^2)^2} \frac{d}{dw} (w^2 u_\theta^*) \right\} - \frac{12u_\theta^*}{w^2(1+w^2)^{4/3}} \right] \delta\tau^{-q-7/3} = 0, \quad (7.9)$$

$$\left(w \frac{du_\theta^*}{dw} + 2qu_\theta^* \right) \delta\tau^{-q-1} + 2\delta_\Phi^* \delta\tau^{-r} = 0, \quad (7.10)$$

and

$$\left[\frac{d}{dw} \left\{ \frac{w^2(1+w^2)^{5/3}}{3+7w^2} \frac{d}{dw} (w^2 \delta_\Phi^*) \right\} - \frac{2w^2(3+7w^2)}{3(1+w^2)^{1/3}} \delta_\Phi^* \right] \delta\tau^{-r+5/3} - \frac{2}{9} w^4 \delta_\rho^* \delta\tau^{-p+2} = 0. \quad (7.11)$$

Since the power of $\delta\tau$ should be balanced in each equation, we obtain

$$q = p - \frac{4}{3} \quad \text{and} \quad r = p - \frac{1}{3}. \quad (7.12)$$

Eqs.(7.9)–(7.11) constitute a closed system of ordinary differential equations. In order to obtain a solution of the above equations, we also need numerical integration. However, here we are going to search for regular and gentle

solutions of the ordinary differential equations. This is much easier than the previous numerical integration of the partial differential equations of which solutions show singular behavior. Further high numerical accuracy is guaranteed and therefore the following analysis might be called “semi-analytic”.

By an appropriate manipulation [32], we obtain a single decoupled equation for u_θ^* as

$$\frac{d^4 u_\theta^*}{dy^4} + c_3 \frac{d^3 u_\theta^*}{dy^3} + c_2 \frac{d^2 u_\theta^*}{dy^2} + c_1 \frac{du_\theta^*}{dy} + c_0 u_\theta^* = 0, \quad (7.13)$$

where $y \equiv w^2$ and

$$\begin{aligned} c_0 = & -2\{-24(9 + 26y + 21y^2) \\ & + 3q^2(63 + 414y + 1016y^2 + 1106y^3 + 441y^4) \\ & + q(252 + 1323y + 3149y^2 + 3465y^3 + 1323y^4)\} \\ & \times \{9y^3(1 + y)^3(3 + 7y)^2\}^{-1}, \end{aligned} \quad (7.14)$$

$$\begin{aligned} c_1 = & \{378 + 2196y + 4758y^2 + 2006y^3 - 4424y^4 - 3234y^5 \\ & + 3q^2(1 + y)^2(189 + 1035y + 1911y^2 + 1225y^3) \\ & + q(1323 + 7893y + 18966y^2 + 21202y^3 + 9247y^4 + 441y^5)\} \\ & \times \{18y^3(1 + y)^3(3 + 7y)^2\}^{-1}, \end{aligned} \quad (7.15)$$

$$\begin{aligned} c_2 = & \{1269 + 7731y + 18453y^2 + 19565y^3 + 7350y^4 + 9q^2(3 + 10y + 7y^2)^2 \\ & + 6q(153 + 993y + 2387y^2 + 2527y^3 + 980y^4)\} \\ & \times \{9y^2(1 + y)^2(3 + 7y)^2\}^{-1}, \end{aligned} \quad (7.16)$$

$$\begin{aligned} c_3 = & \{159 + 506y + 427y^2 + 12q(3 + 10y + 7y^2)\} \\ & \times \{6y(1 + y)(3 + 7y)\}^{-1}. \end{aligned} \quad (7.17)$$

Giving an appropriate boundary condition, we can numerically solve Eqs.(7.9)–(7.11) as a kind of the eigen value problem to obtain q and the solution for u_θ^* .

The boundary condition at $y = 0$ is given by the following procedure. First, we assume that δ_ρ^* , u_θ^* and δ_Φ^* are C^∞ functions. By this assumption, the perturbation variables are written in the form of the Taylor series as,

$$\delta_\rho^* = \sum_{m=0}^{\infty} \delta_{(m)} y^m, \quad (7.18)$$

$$u_\theta^* = \sum_{m=0}^{\infty} u_{(m)} y^m, \quad (7.19)$$

$$\delta_\Phi^* = \sum_{m=0}^{\infty} \Delta_{(m)} y^m. \quad (7.20)$$

Then substituting the above expressions into Eqs.(4.17)–(4.20), we obtain

$$\delta_{(0)} \left(\frac{4}{3} + q \right) - 32u_{(0)} + 14u_{(1)} = 0, \quad (7.21)$$

$$\delta_{(1)} \left(\frac{7}{3} + q \right) + \frac{1568}{9}u_{(0)} - 104u_{(1)} + 36u_{(2)} = 0, \quad (7.22)$$

$$\delta_{(2)} \left(\frac{10}{3} + q \right) - \frac{18848}{7}u_{(0)} + \frac{1388}{3}u_{(1)} - 208u_{(2)} + 66u_{(3)} = 0, \quad (7.23)$$

$$(q + m)u_{(m)} + \Delta_{(m)} = 0, \quad (7.24)$$

$$-28\Delta_{(0)} + 21\Delta_{(1)} - \delta_{(0)} = 0, \quad (7.25)$$

$$148\Delta_{(0)} - 3(46\Delta_{(1)} - 54\Delta_{(2)} + \delta_{(1)}) = 0, \quad (7.26)$$

$$-\frac{620}{81}\Delta_{(0)} + \frac{119}{18}\Delta_{(1)} - 4\Delta_{(2)} + \frac{11}{2}\Delta_{(3)} - \frac{1}{18}\delta_{(2)} = 0, \quad (7.27)$$

where m is non-negative integer. From the above equations, we obtain

$$u_{(1)} = \frac{4(-24 + 28q + 21q^2)}{21(2 + 7q + 3q^2)}u_{(0)}, \quad (7.28)$$

$$u_{(2)} = \frac{2(5248 + 4822q + 3765q^2 + 2646q^3 + 567q^4)}{567(2 + 7q + 3q^2)(12 + 13q + 3q^2)}u_{(0)}, \quad (7.29)$$

$$u_{(3)} = -\frac{4(2174336 + 3606320q + 2343504q^2 + 889242q^3 + 272511q^4 + 62370q^5 + 6237q^6)}{18711(2 + 7q + 3q^2)(12 + 13q + 3q^2)(28 + 19q + 3q^2)}u_{(0)}. \quad (7.30)$$

Since Eq.(7.13) is linear, the value of $u_{(0)}$ has no special meaning and hence we set $u_{(0)} = 1$, for simplicity. Then the boundary condition at $y = 0$ for Eq.(7.13) is uniquely determined as

$$u_\theta^*|_{y=0} = u_{(0)} = 1, \quad \left.\frac{du_\theta^*}{dy}\right|_{y=0} = u_{(1)}, \quad \left.\frac{d^2u_\theta^*}{dy^2}\right|_{y=0} = 2u_{(2)}, \quad \text{and} \quad \left.\frac{d^3u_\theta^*}{dy^3}\right|_{y=0} = 6u_{(3)}. \quad (7.31)$$

We numerically integrate Eq.(7.13) outward from $y = 0$ by 4th-order Runge-Kutta method. The behavior of u_θ^* depends on the value of q .

In order to set up the boundary condition at the outer numerical boundary, we consider the behavior of Eq.(7.13) in the limit of $y \rightarrow \infty$,

$$\frac{d^4u_\theta^*}{dy^4} + \frac{1}{6y}(12q + 61)\frac{d^3u_\theta^*}{dy^3} + \frac{1}{3y^2}(3q^2 + 40q + 50)\frac{d^2u_\theta^*}{dy^2} + \frac{1}{6y^3}(25q^2 + 3q - 22)\frac{du_\theta^*}{dy} - \frac{6}{y^4}q(q + 1)u_\theta^* = 0. \quad (7.32)$$

Therefore, u_θ^* behaves as

$$u_\theta^* \longrightarrow \text{Const.} \times y^k \quad \text{for} \quad y \longrightarrow \infty. \quad (7.33)$$

Inserting the above equation into Eq.(7.32), we obtain a 4th-order algebraic equation for k . The solutions of this equation are given by

$$k = -q, \quad -(q + 1), \quad -\frac{9}{2} \quad \text{and} \quad \frac{4}{3} \quad (7.34)$$

In order to pick up a solution from the above four independent asymptotic solutions, we consider U_θ^* in the limit of $y \rightarrow \infty$,

$$U_\theta^* \longrightarrow \text{Const.} \times y^k \delta\tau^{-q} = \text{Const.} \times x^{2k} \delta\tau^{-(k+q)}. \quad (7.35)$$

Here we impose a condition that U_θ^* is non-zero and finite for $0 < x < \epsilon$ at $\delta\tau = 0$, where ϵ is a positive infinitesimal number. This condition leads to

$$k = -q. \quad (7.36)$$

Hence by varying q , we search for the solution which behaves

$$u_\theta^* \longrightarrow \text{Const.} \times y^{-q} \quad \text{for} \quad y \longrightarrow \infty. \quad (7.37)$$

The numerical calculation reveals that the above behavior is realized when

$$q = 0.3672. \quad (7.38)$$

From Eq.(7.12), we obtain

$$p = 1.701 \quad \text{and} \quad r = 1.367. \quad (7.39)$$

The above values agree with the numerical results (7.5) quite well. We depict the data for $\delta_\rho^*/\delta_{(0)}$, u_θ^* and $\delta_\Phi^*/\Delta_{(0)}$ in Figs.5, 6 and 7 together with the variables Δ_ρ^\dagger , U_θ^\dagger and Δ_Φ^\dagger obtained by the numerical calculation of Eqs.(6.12)–(6.17), where $\delta_{(0)}$ and $\Delta_{(0)}$ are defined by Eqs.(7.18) and (7.20), respectively. We see the quite excellent agreement.

Now we examine the mass-quadrupole moment $Q(T)$ and its time-derivatives $d^m Q/dT^m$. In order to see the contribution of the central singularity to $d^m Q/dT^m$, we consider the integrand in the right hand side of Eq.(5.5). Using Eqs.(3.22), (3.24) and (7.1), we obtain

$$\begin{aligned} F' \Delta_\rho R^2 &\longrightarrow \frac{4}{3} \tau_{R(1)}^{4/3} w^6 (1+w^2)^{4/3} \delta_\rho^*(w) \delta \tau^{13/3-p} \\ &= \frac{4}{3} \tau_{R(1)}^{4/3} x^{2(13/3-p)} w^{2(p-4/3)} (1+w^2)^{4/3} \delta_\rho^*(w). \end{aligned} \quad (7.40)$$

From the above equation, we obtain

$$\begin{aligned} I^{(m)}(\tau, x) &\equiv \frac{\partial^m}{\partial \tau^m} (F' \Delta_\rho R^2) \longrightarrow \frac{2^{2-m}}{3} \tau_{R(1)}^{4/3-m} \delta \tau^{13/3-p-m} w^{26/3-2p-2m} \\ &\times \left(w^3 \frac{d}{dw} \right)^m \left\{ w^{2(p-4/3)} (1+w^2)^{4/3} \delta_\rho^*(w) \right\}. \end{aligned} \quad (7.41)$$

We consider the integral of $I^{(m)}$ from $x = 0$ to $x = x_o$ to see the contribution of the central shell focusing naked singularity to the time derivatives of the mass-quadrupole moment. Here we take a limit $\delta \tau \rightarrow 0$ with fixed $w_o \equiv x_o \delta \tau^{-1/2}$ and then consider the limit $w_o \rightarrow \infty$. As a result, we obtain

$$\begin{aligned} \int_0^{x_o} I^{(m)}(\tau, x) dx &= \delta \tau^{1/2} \int_0^{w_o} I^{(m)}(\tau, \delta \tau^{1/2} w) dw \\ &\longrightarrow \frac{2^{2-m}}{3} \tau_{R(1)}^{4/3-m} \delta \tau^{29/6-p-m} \\ &\times \int_0^\infty w^{26/3-2p-2m} \left(w^3 \frac{d}{dw} \right)^m \left\{ w^{2(p-4/3)} (1+w^2)^{4/3} \delta_\rho^*(w) \right\} dw. \end{aligned} \quad (7.42)$$

The above equation and Eq.(7.39) show that the contribution of the central singularity to $d^m Q/dT^m$ diverges for $\tau \rightarrow 1$ if and only if m is larger than or equal to 4. This result and the quadrupole formula imply that the metric perturbation corresponding to the gravitational radiation and its first order temporal derivative is finite but the second order temporal derivative diverges. Hence the power L_{GW} of the gravitational radiation is finite but the curvature Ψ_4 carried by the gravitational waves from the central naked singularity diverges; see Eqs.(5.6) and (5.7). This agrees with the relativistic perturbation analysis. Further, we find that in the limit of $\tau \rightarrow 1$,

$$\Psi_4 = -\frac{3\pi}{5} \frac{d^4 Q}{dT^4} \propto \delta \tau^{5/6-p} \propto (1-\tau)^{-0.867}. \quad (7.43)$$

This result is also consistent with the relativistic perturbation analysis [24].

VIII. SUMMARY AND CONCLUDING REMARKS

We analyzed the even mode perturbations of $l = 2$ in the spherically symmetric dust collapse in the framework of the Newtonian approximation and estimated the gravitational radiation generated by these perturbations by the quadrupole formula. Since we treat separately the dynamics of the matter perturbations and the gravitational waves in the wave zone, we can estimate the asymptotic behavior semi-analytically, where “semi-analytically” means that we know it by solving the gentle ordinary differential equations. This is the great advantage of the Newtonian approximation.

As a result, we found that the power carried by the gravitational waves from the neighborhood of the naked singularity at the symmetric center is finite. However, the space-time curvature associated to the gravitational waves becomes infinite in accordance with the power law. This result is consistent with recently performed relativistic perturbation analysis by Iguchi et al. [24]. Furthermore, the power index obtained by the Newtonian analysis also agrees with the relativistic perturbation analysis quite well.

The agreement between the results of the Newtonian and relativistic analyses implies that the perturbations themselves are always confined within the range to which the Newtonian approximation is applicable. Here we will focus on the metric perturbation, Δ_Φ^* . Since the asymptotic solution of Δ_Φ^* has the same form as Eq.(3.33), we immediately find that in the limit of $\delta \tau \rightarrow 0$ with fixed w ,

$$\frac{\partial_T \Delta_\Phi^*}{\partial_R \Delta_\Phi^*} \propto \delta\tau^{1/6}, \quad (8.1)$$

and hence the assumption $|\partial_T \Delta_\Phi^*| \ll |\partial_R \Delta_\Phi^*|$ of the Newtonian approximation is valid in the Eulerian coordinate system. We can also see 2nd-order derivatives. In the same limit, we find

$$\frac{\partial_T \partial_R \Delta_\Phi^*}{\partial_R^2 \Delta_\Phi^*} \propto \delta\tau^{1/6} \quad \text{and} \quad \frac{\partial_T^2 \Delta_\Phi^*}{\partial_R \partial_T \Delta_\Phi^*} \propto \delta\tau^{1/6}. \quad (8.2)$$

From the above equations, we obtain

$$\frac{\partial_T^2 \Delta_\Phi^*}{\partial_R^2 \Delta_\Phi^*} \propto \delta\tau^{1/3}. \quad (8.3)$$

The above equation means that in the limit of $\delta\tau \rightarrow 0$ with fixed w , the following inequality is also satisfied,

$$|\partial_T^2 \Delta_\Phi^*| \ll |\partial_R^2 \Delta_\Phi^*|. \quad (8.4)$$

The above inequality implies that the wave equation for the metric perturbation Δ_Φ is well approximated by the Poisson-type equation if we adopt the Eulerian coordinate system.

However as mentioned in Sec.2, the gravitational collapse producing the shell focusing globally naked singularity is not Newtonian in ordinary sense. The same is true for the perturbation variables because $|\Delta_\Phi/\Delta'_\Phi| \gg 1$ in the limit of $\delta\tau \rightarrow 0$ with fixed w . Even though the Newtonian approximation is valid for the Eulerian coordinate system, the Newtonian order counting breaks down if we adopt the Lagrangian coordinate system as the spatial coordinates.

Acknowledgements

We are grateful to H. Sato for his continuous encouragement. We are also grateful to T. Nakamura, H. Kodama, T.P. Singh, A. Ishibashi and S.S. Deshingkar for helpful discussions. This work was supported by the Grant-in-Aid for Scientific Research (No. 05540) and for Creative Basic Research (No. 09NP0801) from the Japanese Ministry of Education, Science, Sports and Culture.

-
- [1] R. Penrose, Phys. Rev. Lett. **14**, 57 (1965).
 - [2] S. W. Hawking, Proc. R. Soc. London **A300**, 187 (1967).
 - [3] S. W. Hawking and R. Penrose, Proc. R. Soc. London **A314**, 529 (1970).
 - [4] R. Penrose, Riv. Nuovo Cim. **1**, 252 (1969).
 - [5] D.M. Eardley and L. Smarr, Phys. Rev. D **19**, 2239 (1979).
 - [6] D. Christodoulou, Commun. Math. Phys. **93**, 171 (1984).
 - [7] R.P.A.C. Newman, Class. Quantum Grav. **3**, 527 (1986).
 - [8] P.S. Joshi and I.H. Dwivedi, Phys. Rev. D **45**, 5357 (1993).
 - [9] T.P. Singh and P.S. Joshi, Class. Quantum Grav. **13**, 559 (1996).
 - [10] S. Jhingan, P.S. Joshi and T.P. Singh, Class. Quantum Grav. **13**, 3057 (1996).
 - [11] A. Ori and T. Piran, Gen. Relativ. Gravit. **20**, 7 (1988).
 - [12] A. Ori and T. Piran, Phys. Rev. D **42**, 1068 (1990).
 - [13] T. Harada, Phys. Rev. D **58**, 104015 (1998).
 - [14] T. Harada, H. Iguchi and K. Nakao, Phys. Rev. D **58**, 104015 (1998).
 - [15] T. Nakamura, K. Maeda, S. Miyama and M. Sasaki, *Proceedings of the 2nd Marcel Grossmann Meeting on General Relativity* edited by R. Ruffini (Amsterdam: North-Holland), p675 (1982).
 - [16] T. Nakamura and H. Sato, Prog. Theor. Phys. **67**, 1396 (1982).
 - [17] K.S. Thorne, in *Magic Without Magic; John Archibald Wheeler*, edited by J.Klauder (Frieman, San Francisco, 1972), p231. **58**, 104015 (1998).
 - [18] S. L. Shapiro and S. A. Teukolsky, Phys. Rev. Lett. **66**, 994 (1991).
 - [19] A. M. Abrahams and C. R. Evans, Phys. Rev. Lett. **70**, 2980 (1993).
 - [20] P. S. Joshi and A. Krolak, Class. and Quantum Grav. **13**, 3969 (1996).
 - [21] P. Hübner, Phys. Pev. **D53**, 701 (1996).
 - [22] T. Nakamura, M. Shibata and K. Nakao, Prog. Theor. Phys. **89**, 821 (1993).

- [23] T. Chiba, Prog. Theor. Phys. **95**, 321 (1996).
- [24] H. Iguchi, T. Harada and K. Nakao, Prog. Theor. Phys. **103**, 53 (2000)
- [25] S. Barve, T.P. Singh, C. Vaz and L. Witten, Nucl. Phys. B **532**, 361 (1998).
- [26] S. Barve, T.P. Singh, C. Vaz and L. Witten, Phys. Rev. D **58**, 104018 (1998).
- [27] C. Vaz and L. Witten, Phys. Lett. B **442**, 90 (1998).
- [28] T. Harada, H. Iguchi and K. Nakao, Phys.Rev.**D61**, 101502(R) (2000).
- [29] T. Harada, H. Iguchi and K. Nakao, Phys.Rev.**D** in press.
- [30] R. M. Wald, *General Relativity* (The University of Chicago Press, 1984).
- [31] S.A. Hayward, Phys. Rev. **D53**, 1938 (1996)
- [32] In order to avoid miss calculations, we have used the *Mathematica*.

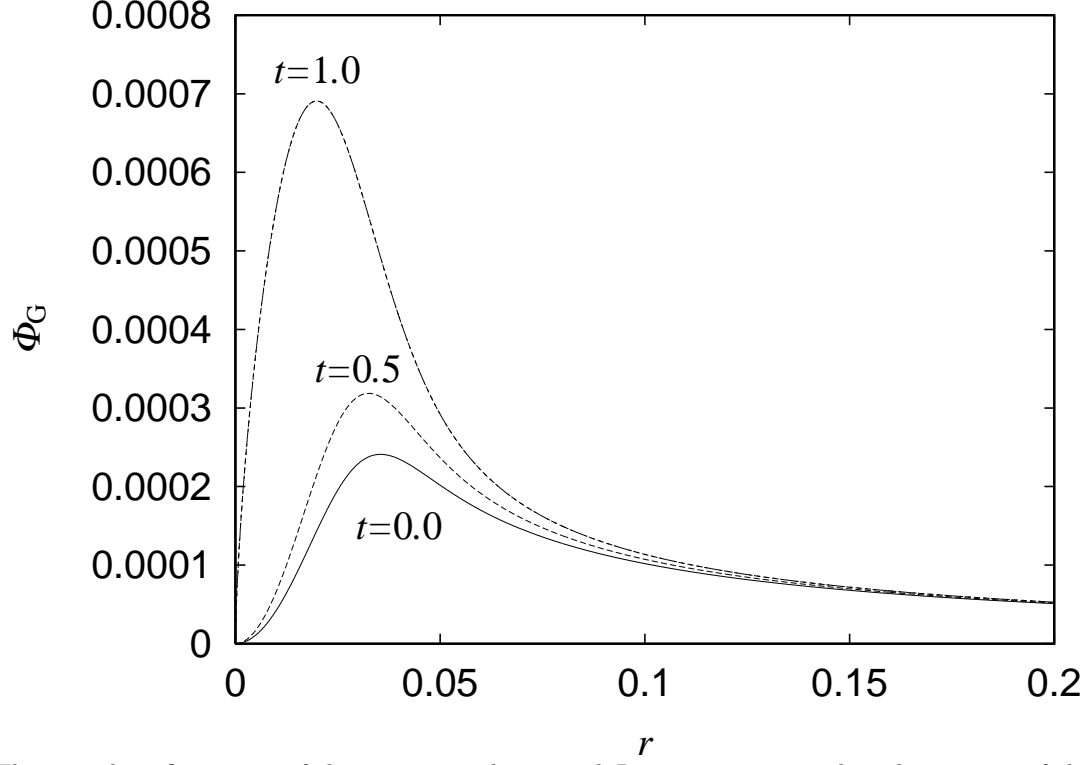
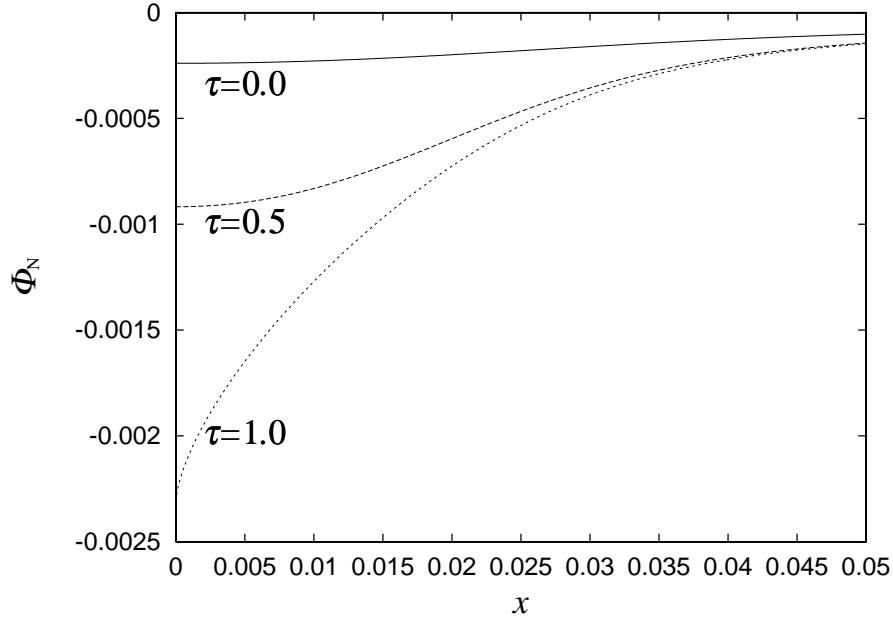
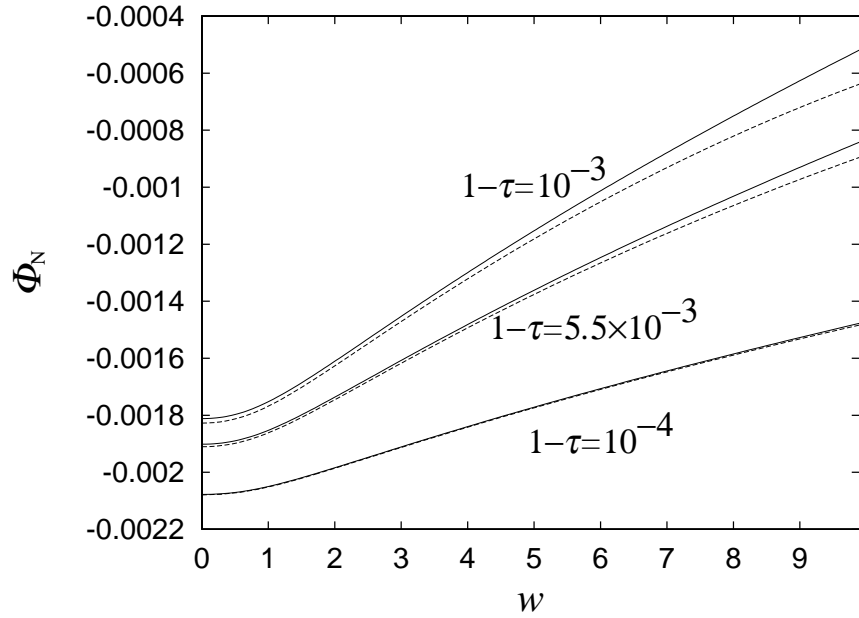


FIG. 1. The spatial configurations of the gravitational potential Φ_G at $t = 0, 0.5$ and at the moment of the central shell focusing singularity formation $t = 1$ are plotted. In all the cases, the gravitational potential Φ_G is everywhere much smaller than unity.



(a)



(b)

FIG. 2. (a) The spatial configurations of the numerically obtained Newtonian gravitational potential Φ_N are plotted as a function of x . The solid line represents Φ_N at $\tau = 0$, while the dashed line corresponds to the case at $\tau = 0.95$. The dotted line represents the case at the central shell focusing singularity formation $t = 1$. Although the regularity of Φ_N at the origin breaks down at $t = 1$, $|\Phi_N|$ is everywhere much smaller than unity. (b) The asymptotic behavior of the Newtonian gravitational potential Φ_N is plotted as a function of w for $\tau = 0.999$ (the top), $\tau = 0.99945$ (the middle) and $\tau = 0.9999$ (the lowest). The solid lines represent Φ_N obtained by the asymptotic analysis (3.32) while dashed lines is the numerically obtained ones. In all the cases, numerically obtained values well agree with those obtained by the asymptotic analysis.

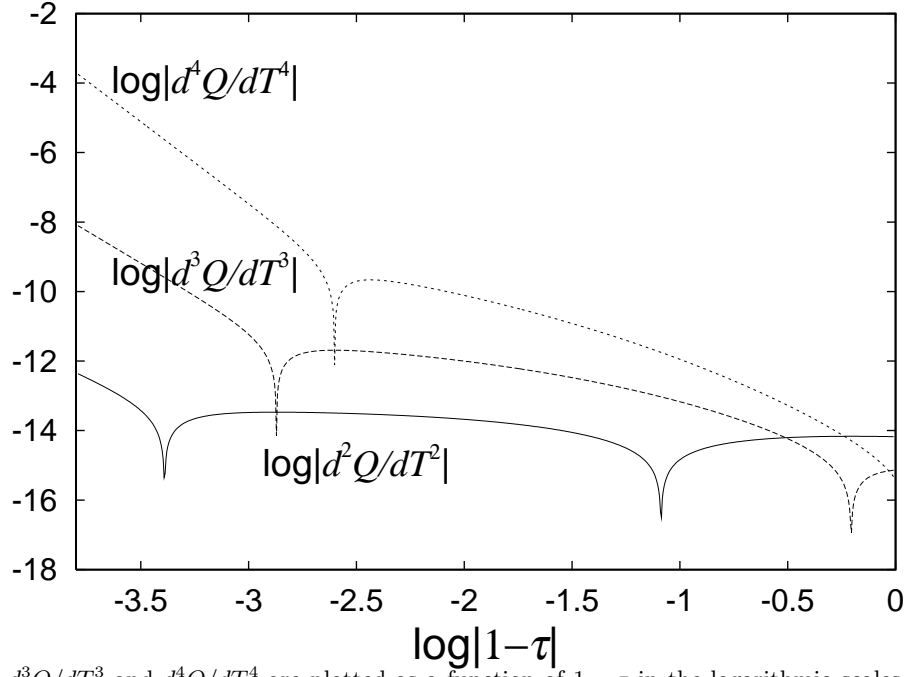


FIG. 3. d^2Q/dT^2 , d^3Q/dT^3 and d^4Q/dT^4 are plotted as a function of $1 - \tau$ in the logarithmic scales. The absolute values of these quantities show oscillatory behavior and grow. At this stage, the contribution near the origin is not dominant.

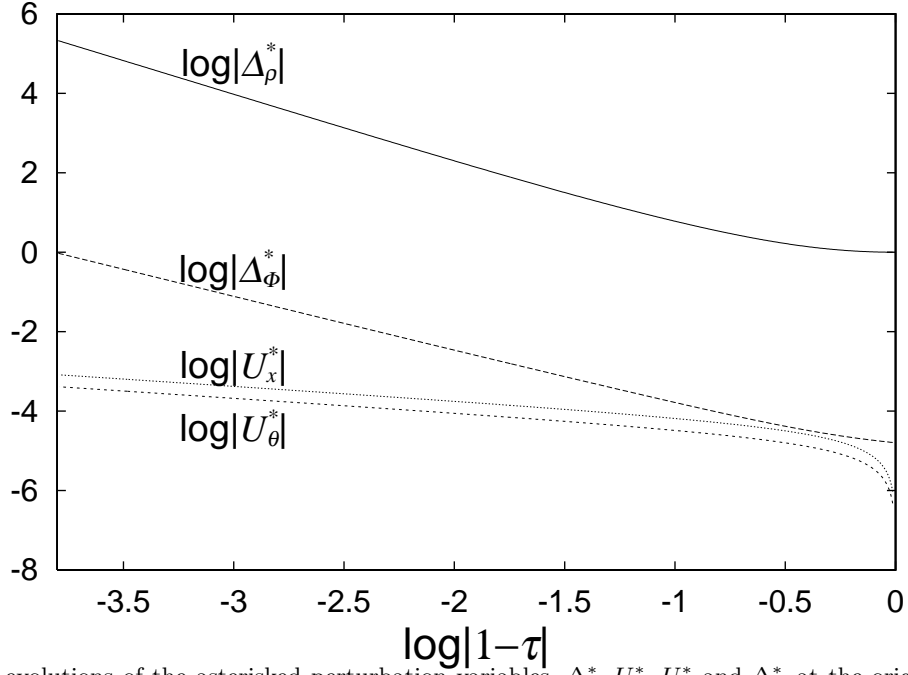


FIG. 4. The time evolutions of the asterisked perturbation variables, Δ_ρ^* , U_x^* , U_θ^* and Δ_Φ^* at the origin are plotted in the logarithmic scales. All these quantities monotonically grow asymptotically in accordance with the power law.

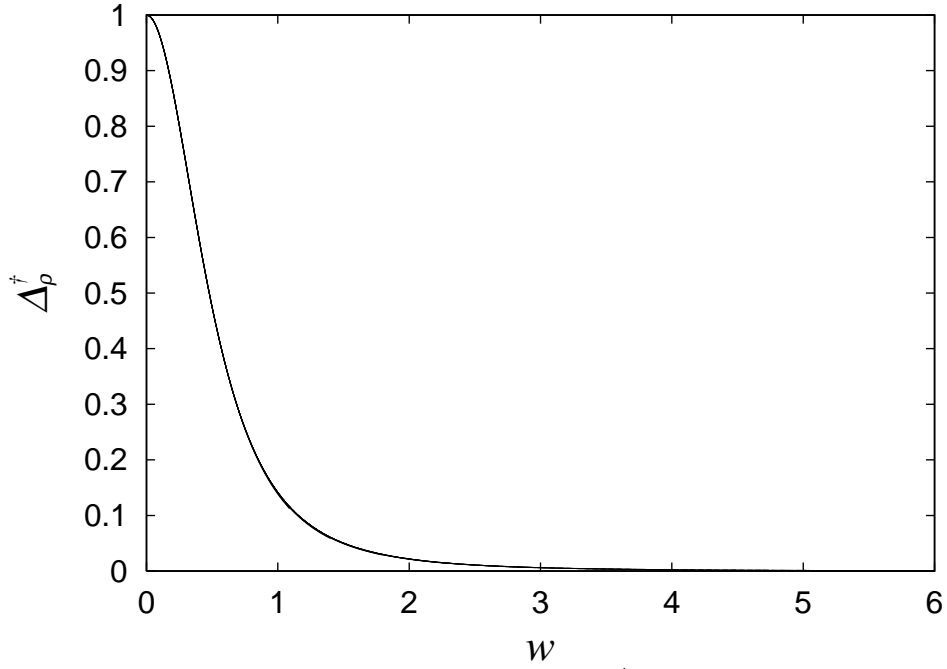


FIG. 5. Spatial configurations of the normalized density perturbation Δ_ρ^\dagger are plotted as a function of w for $x < 0.05x_{\text{core}}$ at various time step from $1 - \tau = 6.6 \times 10^{-3}$ to $1 - \tau = 2.0 \times 10^{-4}$ by solid lines. The density perturbation becomes about 381 times during this time interval. On the other hand, $\delta_\rho^*(w)/\delta_{(0)}$ obtained by the asymptotic estimate is represented by a dashed line. It is very difficult to distinguish these lines from each other.

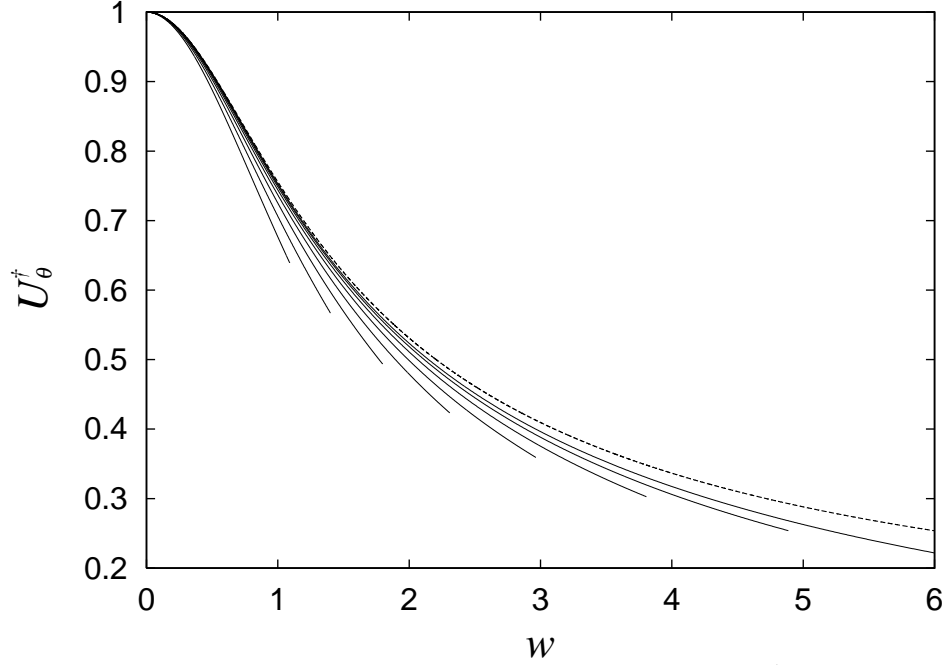


FIG. 6. Spatial configurations of the normalized tangential velocity perturbation U_θ^\dagger are plotted as a function of w for $x < 0.05x_{\text{core}}$ at various time step from $1 - \tau = 6.6 \times 10^{-3}$ to $1 - \tau = 2.0 \times 10^{-4}$ by solid lines. On the other hand, $u_\theta^*(w)$ obtained by the asymptotic estimate is represented by a dashed line. We can see that U_θ^\dagger asymptotically approaches to u_θ^* .

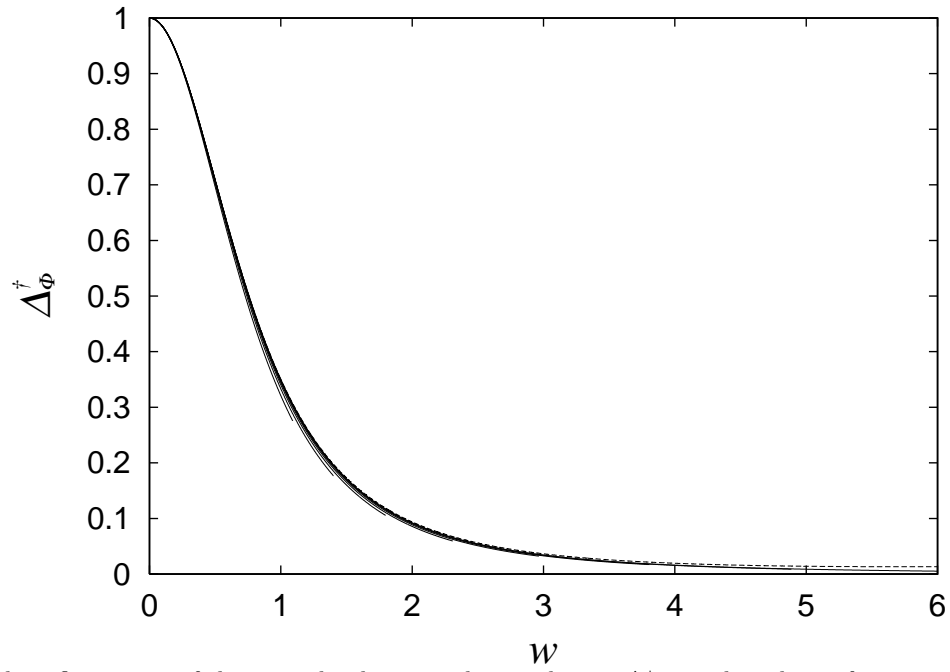


FIG. 7. Spatial configurations of the normalized potential perturbation Δ_{Φ}^* are plotted as a function of w for $x < 0.05x_{\text{core}}$ at various time step from $1 - \tau = 6.6 \times 10^{-3}$ to $1 - \tau = 2.0 \times 10^{-4}$ by solid lines. On the other hand, $\delta_{\Phi}^*(w)/\Delta_{(0)}$ obtained by the asymptotic estimate is represented by a dashed line. The normalized potential perturbation Δ_{Φ}^{\dagger} asymptotically approaches to $\delta_{\rho}^*/\delta_{(0)}$.